



## Optical transitions in InGaN/AlGaIn single quantum wells

K. C. Zeng, M. Smith, J. Y. Lin, H. X. Jiang, J. C. Robert, E. L. Piner, F. G. McIntosh, S. M. Bedair, and J. Zavada

Citation: *Journal of Vacuum Science & Technology B* **15**, 1139 (1997); doi: 10.1116/1.589428

View online: <http://dx.doi.org/10.1116/1.589428>

View Table of Contents: <http://scitation.aip.org/content/avs/journal/jvstb/15/4?ver=pdfcov>

Published by the AVS: Science & Technology of Materials, Interfaces, and Processing

---



## Re-register for Table of Content Alerts

Create a profile.



Sign up today!



# Optical transitions in InGaN/AlGaIn single quantum wells

K. C. Zeng, M. Smith, J. Y. Lin, and H. X. Jiang<sup>a)</sup>

*Department of Physics, Kansas State University, Manhattan, Kansas 66506-2601*

J. C. Robert, E. L. Piner, F. G. McIntosh, and S. M. Bedair

*Department of Electrical and Computer Engineering, North Carolina State University, Raleigh, North Carolina 27685-7911*

J. Zavada

*U. S. Army Research Office, P.O. Box 12211, Research Triangle Park, North Carolina 27709-2211*

(Received 12 January 1997; accepted 23 March 1997)

The optical transitions in InGaN/AlGaIn single quantum wells (SQWs) grown by metal-organic chemical vapor deposition have been studied. The spectral lineshape and the recombination dynamics of the optical transitions have been systematically investigated at different conditions. It was found that the main photoluminescence (PL) emission line in these SQW was contributed predominantly by the localized exciton recombination. However, time-resolved PL results revealed the presence of a band-to-impurity transition which cannot be resolved spectroscopically from the localized exciton transition line due to the broad emission linewidth. © 1997 American Vacuum Society. [S0734-211X(97)08604-6]

## I. INTRODUCTION

The group III-nitride wide band gap semiconductors have attracted much attention recently because of their potential for many applications such as blue/UV light emitting diodes (LEDs), laser diodes (LDs), and high-temperature and high-power electronic devices.<sup>1</sup> In particular, InGaN has the advantage of tunability of the energy gap, allowing greater control over the spectrum of emitted light from visible to near UV. InGaN/AlGaIn single quantum wells (SQWs) are being used as an active medium for commercial high brightness blue/green LEDs.<sup>2</sup> Blue/UV LDs operating at room temperature based on multiple quantum wells (MQW) of  $\text{In}_x\text{Ga}_{1-x}\text{N}/\text{In}_y\text{Ga}_{1-y}\text{N}$  ( $x > y$ ) have also been demonstrated recently.<sup>3</sup> However, the optical properties of InGaN and the nature of the optical transitions in InGaN QWs are not well understood. Needless to say, a better understanding of optical transitions in InGaN QWs is needed for the improvements of optoelectronic devices based on these materials. In this work, we have employed time-resolved photoluminescence (PL) measurements to study the mechanisms of optical transitions in InGaN/AlGaIn SQW. Compared with InGaN/GaN and GaN/AlGaIn QW structures,<sup>4</sup> the InGaN/AlGaIn QW structure provides more controlled parameters due to the fact that both the barrier and well materials are alloys, an enhanced photon confinement due to the larger difference in the indices of refraction between InGaN and AlGaIn, and an enhanced carrier confinement due to the larger band offset.

## II. SAMPLES

Unintentionally doped InGaN/AlGaIn SQW samples used here were grown by metal organic chemical vapor deposition (MOCVD) in an atmospheric pressure vertical reactor. The structure of these InGaN/AlGaIn SQW is shown schemati-

cally in Fig. 1. Source gases used were ammonia ( $\text{NH}_3$ ), trimethylgallium (TMG,  $-10^\circ\text{C}$ ), and trimethylaluminum (TMA,  $+18^\circ\text{C}$ ) and ethyldimethylindium (EdMIn,  $+10^\circ\text{C}$ ) was used as the carrier gas. Prior to the deposition of the SQW, a thin 100 Å AlN buffer layer was grown on a (0001) sapphire substrate at  $700^\circ\text{C}$  by atomic layer epitaxy (ALE). Next, a 0.1- $\mu\text{m}$ -thick  $\text{Al}_y\text{Ga}_{1-y}\text{N}$  ( $y \sim 0.05$ ) cladding layer was grown by MOCVD at  $950^\circ\text{C}$ , followed by a graded  $\text{In}_x\text{Ga}_{1-x}\text{N}$  layer deposited while the temperature was ramped down from  $800$  to  $750^\circ\text{C}$ . The active  $\text{In}_x\text{Ga}_{1-x}\text{N}$  was then grown at  $750^\circ\text{C}$ , followed by a 500 Å  $\text{Al}_y\text{Ga}_{1-y}\text{N}$  ( $y \sim 0.05$ ) upper cladding layer grown at  $950^\circ\text{C}$  to complete the structure. The thickness of the active  $\text{In}_x\text{Ga}_{1-x}\text{N}$  well is estimated to be about 50 Å, based on the growth rate and the transmission electron microscope (TEM) studies carried out on this material system. The value of  $x$  was estimated in the 20%–25% range as determined by x-ray diffraction studies on thicker  $\text{In}_x\text{Ga}_{1-x}\text{N}$  films. This range in the value of  $x$  is due to compositional nonuniformity across the wafer in our current ALE/MOCVD reactor. From these parameters, the energy band diagram of the InGaN/AlGaIn single quantum well sample studied here can be constructed and is shown in Fig. 2.

## III. EXPERIMENT

For photoluminescence measurements, samples were attached to copper sample holders and placed inside a closed-cycle He refrigerator with a temperature variation from 10 to 320 K. A temperature controller enabled us to stabilize the temperature to within 0.1 K. Photoluminescence spectra were collected in a reflecting mode. Excitation pulses of about 7 ps at a repetition rate of 9.5 MHz were provided by a cavity-dumped dye laser (Coherent 702-2CD) with Rhodamine 6G dye solution, which was pumped by an yttrium-aluminum-garnet (YAG) laser (Coherent Antares 76) with a frequency doubler. The output from the dye laser was

<sup>a)</sup>Electronic mail: Jiang@Phys.ksu.edu

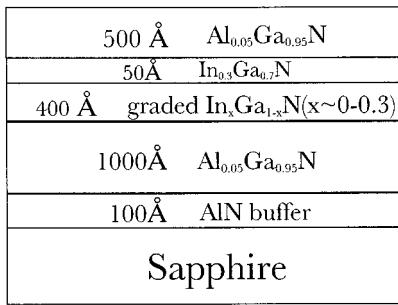


FIG. 1. Schematic diagram of MOCVD grown InGaN/AlGaIn single quantum well samples used in this work.

frequency doubled again by a second frequency doubler to provide tunability in the UV region. The laser output after the second doubler has an average power of about 20 mW, a tunable photon energy up to 4.5 eV, and a spectral width of about 0.2 meV. The laser beam size on the sample was about 0.3 mm in diameter. A single photon counting detection system was used to record the time-resolved photoluminescence spectra. With the use of a microchannel-plate photomultiplier tube (MCP-PMT), the overall time resolution of the detection system was about 20 ps. The excitation intensity was controlled by a set of UV neutral density filters with different attenuation parameters *D*, and was thus proportional to 10<sup>-D</sup>.

**IV. RESULTS AND DISCUSSIONS**

Figure 3 shows the continuous-wave (cw) photoluminescence (PL) emission spectra of an InGaN/AlGaIn SQW measured at *T*=10 K. The main peak at about 2.8 eV results from the InGaN active well region and is predominantly due to the localized exciton recombination. An additional emission line with a much lower emission intensity and a narrower linewidth at about 3.62 eV is also evident in Fig. 1, which results from optical recombination in the Al<sub>y</sub>Ga<sub>1-y</sub>N barrier layers. This assignment is based on the fact that the emission energy is consistent with the expected Al composition of about 0.05.

Figure 4 shows the cw PL spectra measured at *T*=10 K for five representative excitation intensities, *I*<sub>exc</sub>=0.01, 0.1, 0.32, 0.63, and 1.0 *I*<sub>0</sub>,

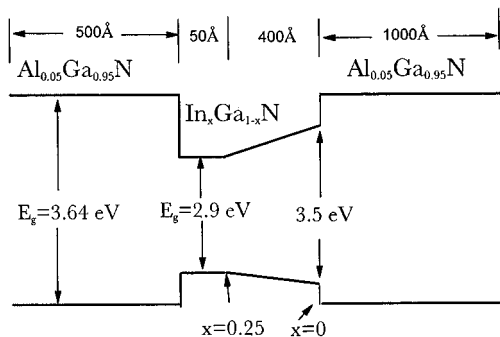


FIG. 2. Energy band diagram of InGaN/AlGaIn single quantum well sample used here.

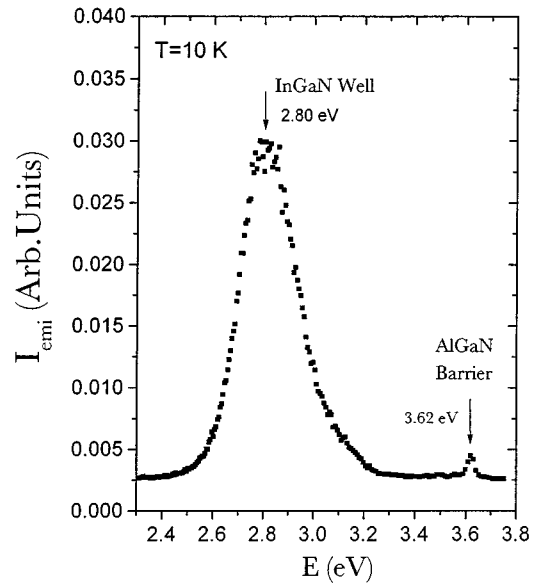


FIG. 3. PL spectrum of an InGaN/AlGaIn SQW measured at 10 K.

0.32, 0.63, and 1.0 *I*<sub>0</sub>. These spectra have been normalized to the maximum peak intensity for each *I*<sub>exc</sub> for a better illustration. The overall spectral line shapes for different *I*<sub>exc</sub> are quite similar. However, it is clear that the peak position of the dominant band is shifted toward higher energies as excitation intensity increases. This observation is expected for a localized exciton recombination. In semiconductor alloys, excitons are localized in random potential wells induced by alloy disorder. At higher excitation intensities, lower energy

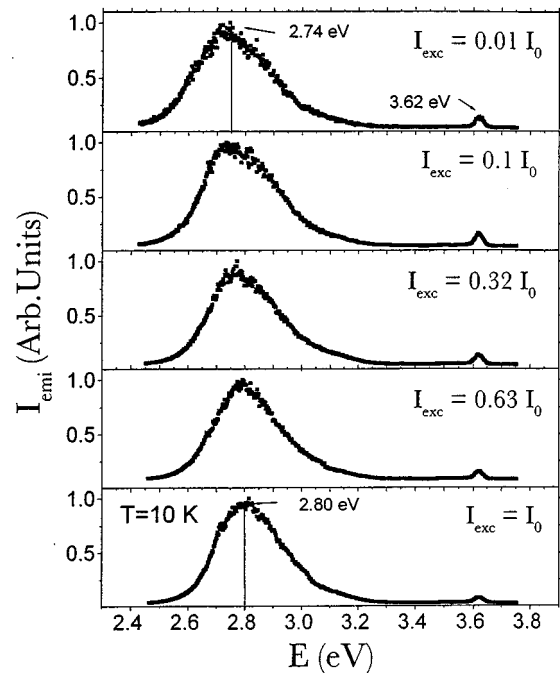


FIG. 4. PL spectra measured at *T*=10 K for five representative excitation intensities, *I*<sub>exc</sub>=0.01, 0.1, 0.32, 0.63, and 1.0 *I*<sub>0</sub>, respectively.

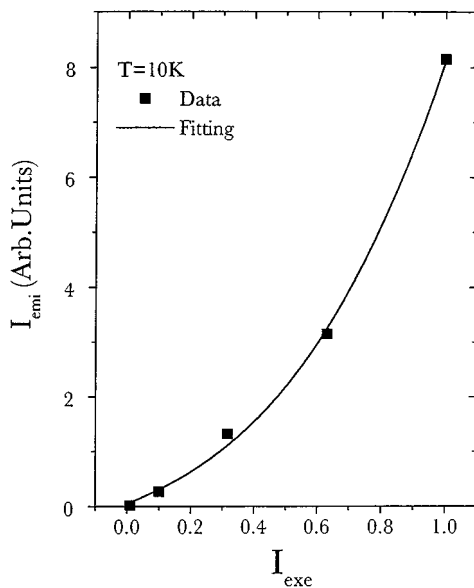


FIG. 5. Excitation intensity dependence of PL emission intensity measure at 10 K. The solid curve is the least squares fit of data by Eq. (1).

states are more likely being occupied and consequently more excitons have to fill in higher energy states, which causes the shift of emission peak position toward the higher energies.

The PL emission intensity,  $I_{\text{emi}}$ , of the dominant PL band near 2.8 eV at 10 K as a function of excitation intensity,  $I_{\text{exc}}$ , has been measured. This is plotted in Fig. 5. It is found that  $I_{\text{emi}}$  increases superlinearly with excitation intensity,  $I_{\text{exc}}$ , following a power-law form,

$$I_{\text{emi}} \propto I_{\text{exc}}^{\beta}. \quad (1)$$

The solid curve in Fig. 5 is the least squares fit of the data with Eq. (1), where the fitted exponent  $\beta$  is about 1.4. The superlinear increase of  $I_{\text{emi}}$  with  $I_{\text{exc}}$  has also been observed for the localized exciton recombination in InGaIn epilayers,<sup>5</sup> in which the exponent  $\beta$  is 2.6. The superlinear behavior seen here supports our interpretation that the main emission line in these InGaIn SQW is of a predominantly intrinsic nature, i.e., localized exciton recombination. The smaller value of exponent  $\beta$  seen here may be due to the presence of an impurity related transition which cannot be resolved spectroscopically from the localized exciton transition line due to the broad linewidth.

In order to elucidate further the nature of the dominant emission line near 2.8 eV in InGaIn/AlGaIn SQW, we have employed a time-resolved PL to study its dynamical behavior. There have been a few prior measurements on time-resolved PL on similar systems, such as InGaIn epilayers<sup>5</sup> and InGaIn/GaN SQW.<sup>6-8</sup> The decay of the localized excitons in high-quality InGaIn epilayers is exponential, while the PL in InGaIn/GaN SQW under a strong excitation decays according to a bimolecular law due to the nature of the band-to-band (free electron-to-free hole) transition under such a condition. On the contrary, the decay of the PL emission band in InGaIn/AlGaIn SQW observed here is neither an exponential nor a bimolecular type. This is illustrated in Fig. 6

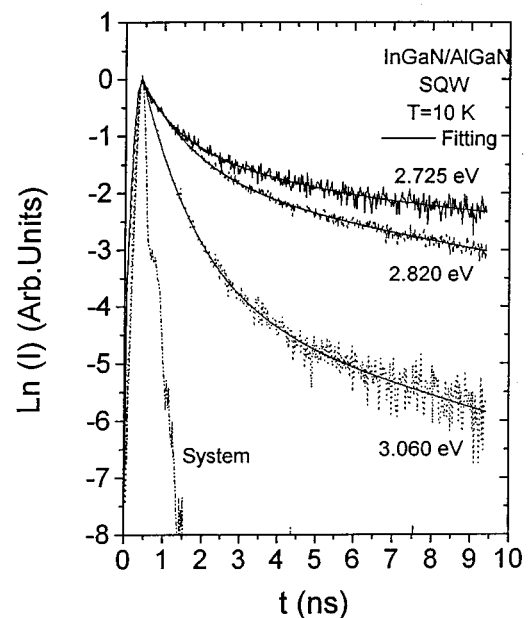


FIG. 6. Semilogarithmic plot of PL temporal responses measured at three representative emission energies. The solid curves are the least squares fit of data by two-exponential decay functions of Eq. (2). The detection system response ( $\sim 20$  ps) to the laser pulses (7 ps) is indicated as “system.”

where the temporal responses of PL emission measured at 10 K for three representative emission energies together with a system response (20 ps) to the laser pulses are shown. The PL decay shown in Fig. 6 can be described very well by a two-exponential function,

$$I(t) = A_1 \exp(-t/\tau_1) + A_2 \exp(-t/\tau_2), \quad (2)$$

where  $\tau_1$  and  $\tau_2$  are the recombination lifetimes for the faster and slower components, respectively. Across the entire emission band, PL decay kinetics can all be fit very well by Eq. (2) and the PL amplitude of the fast decay component  $A_1$  is always greater than 90%.

In Fig. 7, we plot the recombination lifetimes of the fast and slow decay components,  $\tau_1$  and  $\tau_2$ , as functions of emission energy.  $\tau_1$  is approximately constant in the range from 2.67 to 2.8 eV and then decreases from 0.7 to 0.4 ns as the emission energy increases from 2.8 to 3.05 eV and is comparable to the recombination lifetimes of the localized excitons in InGaIn epilayers.<sup>5</sup> Localized excitons in semiconductor alloys can transfer from higher energy sites to lower energy sites with a relaxation rate that increases with an increase of emission energy.<sup>6</sup> Thus the observed decrease of  $\tau_1$  with increasing emission energy shown in Fig. 7(a) is also expected for localized excitons. These results further support our interpretation that the main emission band in InGaIn SQW is contributed predominantly by the localized exciton recombination. However, there is a second PL emission component ( $A_2 < 10\%$ ) which has a recombination lifetime ( $\tau_2$ ) ranging from 5.5 to 2.5 ns. The observed nanosecond recombination lifetimes of  $\tau_2$  suggests that this second emission component is of a band-to-impurity nature. Addition-

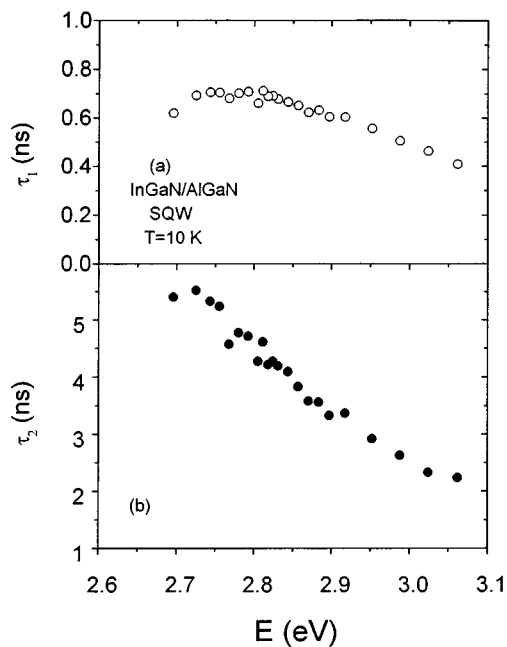


FIG. 7. The emission energy dependence of (a) the fast recombination lifetime,  $\tau_1$ , and (b) the slow recombination lifetime,  $\tau_2$ .

ally, the emission energy dependence of the recombination lifetime  $\tau_2$  is also similar to that of a band-to-impurity transition seen previously in a GaN epilayer.<sup>9</sup>

Furthermore, based on a previous theoretical model,<sup>10</sup> the asymptotic decay of the band-to-impurity recombination at longer times follows a power law,  $I(t) \propto t^{-\alpha}$ . We have replotted PL temporal responses in a double logarithmic scale and found that the PL decay at longer times indeed follows a power law with the decay exponent  $\alpha$  increasing with an increasing of the emission energy. A power law decay at longer times has been observed for a band-to-impurity recombination in *p*-type doped GaN previously.<sup>11</sup> This further supports our interpretation that the second slower decay component is due to a band-to-impurity recombination.

Finally, we have also obtained some preliminary results on recently grown InGaN/AlGaIn SQW of higher quality, in which more than one emission peak can be clearly resolved in time-resolved PL spectra. This further corroborates our assignment. The dependence of  $\tau_2$  on emission energy at low temperatures suggests that the energy level of the impurity involved in the transition may have a distribution, which together with alloy disorder in InGaN causes the broad emission linewidth observed in the SQW investigated here. Additionally, interface roughness, dislocations caused by lattice and thermal coefficient mismatches between InGaN and AlGaIn, and native defects may also contribute to the emission linewidth broadening, which further leads to the difficulties in resolving different emission lines in cw PL spectra.

The excitation intensity dependencies of the recombination lifetimes  $\tau_1$  and  $\tau_2$  have also been measured and are shown in Fig. 8. Both  $\tau_1$  and  $\tau_2$  are almost constants when  $I_{\text{exc}}$  is varied by two orders of magnitude. This suggests that the localized exciton recombination is always the dominant

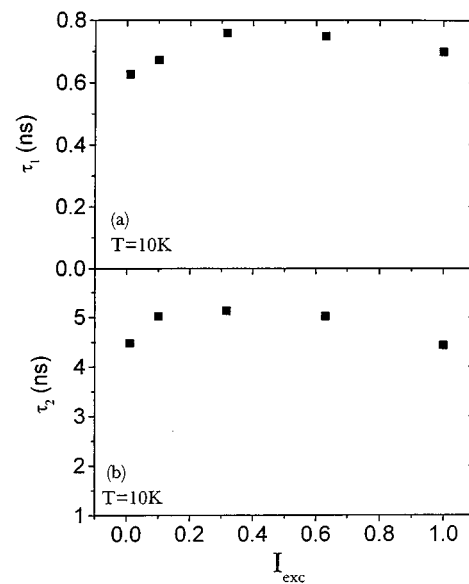


FIG. 8. Excitation intensity dependencies of the recombination lifetimes  $\tau_1$  and  $\tau_2$  measured at the spectral peak positions at 10 K.

optical transition in InGaN/AlGaIn SQW samples studied here.

## V. SUMMARY

Mechanisms of optical transitions of InGaN/AlGaIn SQW have been studied by time-resolved PL under different conditions. The dynamical behavior of the PL emission reveals that the main emission line in these SQW is due to the combination of the localized exciton and a band-to-impurity recombination. The spectral line shape and the recombination dynamics of the localized exciton and the band-to-impurity transitions have been systematically investigated at different conditions.

## ACKNOWLEDGMENTS

The research at Kansas State University is supported by ARO (DAAH04-96-1-0371), BMDO/ONR (N00014-96-1-0885), and NSF (DMR-95-28226). The research at North Carolina State University is supported by ARO (DAAH04-96-1-0173) and ONR (N00014-92-J-1473).

<sup>1</sup>H. Morkoc, S. Strite, G. B. Gao, M. E. Lin, B. Sverdlov, and M. Burns, *J. Appl. Phys.* **76**, 1363 (1994).

<sup>2</sup>S. Nakamura, M. Senoh, N. Iwasa, and S. Nagahama, *Jpn. J. Appl. Phys.* **34**, L797 (1995).

<sup>3</sup>S. Nakamura, M. Senoh, N. Iwasa, S. Nagahama, T. Yamada, T. Matsushita, H. Kiyoku, and Y. Sugimoto, *Appl. Phys. Lett.* **68**, 2105 (1996).

<sup>4</sup>M. Smith, J. Y. Lin, H. X. Jiang, A. Salvador, W. Kim, A. Botchkarev, and H. Morkoc, *Appl. Phys. Lett.* **69**, 2453 (1996).

<sup>5</sup>M. Smith, G. D. Chen, J. Y. Lin, H. X. Jiang, M. A. Khan, and Q. Chen, *Appl. Phys. Lett.* **69**, 2837 (1996).

<sup>6</sup>C. K. Sun, S. Keller, G. Wang, M. S. Minsky, J. E. Bowers, and S. P. DenBaars, *Appl. Phys. Lett.* **69**, 1936 (1996).

<sup>7</sup>E. S. Jeon, V. Kozlov, Y. K. Song, A. Vertikov, M. Kuball, A. V. Nurmikko, H. Liu, C. Chen, R. S. Kern, C. P. Kuo, and M. G. Craford, *Appl. Phys. Lett.* **69**, 4194 (1996).

<sup>8</sup>W. Li, P. Bergman, B. Monemar, H. Amano, and I. Akasaki, *J. Appl. Phys.* **81**, 1005 (1997).

<sup>9</sup>G. D. Chen, M. Smith, J. Y. Lin, H. X. Jiang, A. Salvador, B. N. Sverdlov, A. Botchkarev, and H. Morkoc, *J. Appl. Phys.* **79**, 2675 (1996).

<sup>10</sup>P. Avouris and T. N. Morgan, *J. Chem. Phys.* **74**, 4347 (1981).

<sup>11</sup>M. Smith, G. D. Chen, J. Y. Lin, H. X. Jiang, A. Salvador, B. N. Sverdlov, A. Botchkarev, H. Morkoc, and B. Goldenberg, *Appl. Phys. Lett.* **68**, 1883 (1996).